Journal of Immunological Methods 470 (2019) 46–54

Contents lists available at ScienceDirect

Journal of Immunological Methods

journal homepage: www.elsevier.com/locate/jim

Research paper

Isolation and enrichment of mouse insulin-specific CD4$^+$ T regulatory cells

Neda Đedović[a], Verica Paunović[b], Ivana Stojanović[a,*]

[a] Department of Immunology, Institute for Biological Research "Siniša Stanković", University of Belgrade, Belgrade, Serbia
[b] Institute of Microbiology and Immunology, School of Medicine, University of Belgrade, Belgrade, Serbia

ARTICLE INFO

Keywords:
Insulin-specific T regulatory cells (Treg)
Type 1 diabetes (T1D)
Immunoregulation
ex vivo protocol
Expansion

ABSTRACT

Polyclonal T regulatory cells (Treg - CD4$^+$CD25$^+$CD127^{low}Foxp3$^+$) are used in several protocols for the treatment of type 1 diabetes (T1D), multiple sclerosis and graft-*versus* host disease in clinical trials. However, general opinion is that autoantigen-specific Treg could be more efficient in autoimmunity suppression due to their direct effect on pathogenic autoantigen-specific effector T cells. This study describes isolation and expansion of insulin-specific Treg *in vitro*. Insulin-specific Treg are uniformly distributed in lymphoid tissues however their number is extremely low. To enrich the proportion of insulin-specific Treg, pure CD4$^+$ cells were co-cultured with insulin B chain peptide-loaded dendritic cells, isolated from mice that develop T1D spontaneously – NOD mice. Insulin-specific CD4$^+$ cell expansion peaked after 48 h of incubation and was in favour of Treg. These cells were then sorted using insulin peptide-loaded MHC class II tetramers and cultured *in vitro* for 48 h in the presence of TCR stimulators, TGF-β and IL-2. The proportion of gained insulin-specific cells with T regulatory phenotype (CD4$^+$CD25^{high}CD127^{low}GITR$^+$FoxP3$^+$) was in average between 93% and 97%. These cells have shown potent *in vitro* suppressive effect on T effector cells, produced IL-10 and TGF-β and expressed PD-1 and CD39. Further proliferation of these insulin-specific Treg required the presence of dendritic cells, anti-CD3 antibody and IL-2. This study provides new, reproducible experimental design for the enrichment and expansion of insulin-specific Treg that can be used for the cell-based therapy of autoimmunity.

1. Introduction

Therapy of autoimmune diseases with T regulatory cells (Treg) is being exceedingly explored. The role of these Treg is to inhibit autoreactive cells and regain self-tolerance. There is a number of Treg populations that control inflammatory processes and counter-act the development of autoimmune reaction, however, one population (CD4$^+$CD25^{high}CD127$^-$) characterized by the expression of FoxP3 is usually used for the cell therapy (Liu et al., 2006; reviewed in Milward et al., 2017 and Stojanovic et al., 2017). Recent clinical trials (phase I) indicate that treatment of newly-diagnosed diabetic children and adults with *in vitro* expanded polyclonal Treg (cells specific for various antigens) is safe, with no adverse effects and in two cases provided insulin-free period up to 2 years (Marek-Trzonkowska et al., 2012; Marek-Trzonkowska et al., 2014; Bluestone et al., 2015).

In contrast to commonly used polyclonal Treg, antigen-specific Treg provide a number of advantages: lower number of cells needed for the effective therapy, avoidance of general immunosuppression, specific Treg traffic to tissues under inflammation. The usage of antigen-specific Treg is mainly restricted to the transgenic animal models of T1D due to their very low numbers *in vivo*. It was shown that the presence of the antigen is mandatory for the prevention of T1D in NOD mice by Treg (Tonkin et al., 2008). If Treg are polyclonal, *i.e.* they recognize a variety of different antigens, they are less efficient in diabetes prevention in animal models compared to autoantigen-specific Tregs (either used in the BDC2.5 transgenic T1D mouse model or in NOD mice) (Tarbell et al., 2004; Masteller et al., 2005; Tang et al., 2004). Also, greater number of polyclonal Treg is needed for achieving the same effect as with antigen-specific cells. Moreover, this infusion of large numbers of polyclonal Treg significantly increases the potential risk of non-specific immune suppression, such as the transient increase in viral reactivation in patients receiving cord blood-derived Treg (Tang and Lee, 2012). As for the quantity of autoantigen-specific Treg, in some cases, as little as 5000 Treg were sufficient to prevent T1D (Tarbell et al., 2004). It is

Abbreviations: DC, dendritic cells; Treg, T regulatory cells; mDC, mature DC; tolDC, tolerogenic DC; T1D, type 1 diabetes; NOD mice, non-obese diabetic mice; FBS, fetal bovine serum; BSA, bovine serum albumin; InsB$_{9:23}$, insulin B peptide 9:23; CFSE, carboxyfluorescein succinimidyl ester; TCR, T cell receptor; CAR, chimeric antigen receptors

* Corresponding author at: Department of Immunology, Institute for Biological Research "Siniša Stanković", University of Belgrade, Bulevar despota Stefana 142, Belgrade 11060, Serbia.
E-mail address: ivana@ibiss.bg.ac.rs (I. Stojanović).

https://doi.org/10.1016/j.jim.2019.04.011
Received 30 January 2019; Received in revised form 1 April 2019; Accepted 25 April 2019
Available online 27 April 2019

reasonable to assume that the efficacy of these autoantigen-specific Tregs ensues from their direct and specific inhibitory action on autoantigen-specific pathogenic T cells.

Limited efforts were made to exploit the naturally-occurring antigen-specific Treg for *ex vivo* expansion. This study sets up a reproducible protocol for the expansion of insulin-specific Treg isolated from NOD mice. These cells exhibited higher suppressive capacity compared to the polyclonal Treg and was mediated both by cell contact (GITR) and soluble mediators (IL-10 and TGF-β).

2. Material and methods

2.1. Chemicals

Fetal bovine serum (FBS), bovine serum albumin, fraction V (BSA), 5-aza 3′deoxycitidine, Na-pyruvate, β-mercaptoethanol, L-glutamine, HEPES, lipopolysaccharide (LPS) and rapamycine were purchased from (Sigma-Aldrich, MA, USA), RPMI 1640 (Biological Industries USA, Cromwell, CT, USA), RBC Lysis buffer (eBioscience, San Diego, CA, USA), STAT3 inhibitor (SantaCruz Biotechnology, San Diego, CA, USA), acutase (ThermoFisher Scientific, Waltham, MA USA).

2.2. Mice

NOD/Ltj mice were purchased from Charles River (Italy), bred and maintained at the Uniprotect Air Flow Cabinet (ZOONLAB GmbH, Castrop-Rauxel, Germany) at the Institute for Biological Research "Sinisa Stankovic", University of Belgrade with free access to food and water. All animals handling and procedures were approved by the Ethical Committee of the Institute for Biological Research "Sinisa Stankovic", University of Belgrade and were in accordance with the Directive 2010/63/EU (App. No 08-04/15).

2.3. Isolation of lymphocytes

Lymphocytes were isolated from cervical, mesenteric, pancreatic lymph nodes, Peyer's patches and spleen under aseptic conditions. Lymphoid tissue (in PBS + 3% FBS) was pressed through 70 μm mesh, single cell suspension was centrifuged at 550 *g* (5 min) and resuspended in RBC Lysis Buffer. After erythrocyte lysis (5 min, RT, and occasional vortexing), tubes were filled with PBS + 3% FBS and centrifuged at 550 *g* (5 min). Cell pellet was resuspended in PBS + 3%FBS and subjected either to magnetic separation of $CD4^+$ or analysis of insulin-specific effector ($CD4^+CD25^{med}$) or Treg. The cell concentration was measured by trypan blue exclusion assay on LUNA-II™ Automated Cell Counter (Logos Biosystems, Gyeonggi-do, South Korea).

2.4. $CD4^+$ magnetic separation

Lymphocytes (60×10^6) in 600 μl of PBS + 3%FBS were incubated with biotin conjugated anti-mouse CD4 (1:60) (eBioscience) for 15 min on ice with occasional shaking. After washing once with PBS + 3% FBS and once with magnetic bead buffer (PBS + 0.5% BSA + 2 mM EDTA), the cells were resuspended in cold beads buffer containing BD IMag™ Streptavidin Particles Plus - DM (1:20, BD Biosciences, Bedford, MA, USA). $CD4^+$ cells were purified by placement in a BD IMag™ Cell Separation Magnet (BD Biosciences), 3× for 8 min, and finally resuspended in a T lymphocyte medium – X-VIVO™ 15 Hematopoietic Cell Medium| (Lonza Biologics, Manchester, UK) supplemented with 10% FCS, 1% penicillin and streptomycin, 0.02 mM Na-pyruvate and 5 μM β-mercaptoethanol. The yield was 95.2 ± 2.1% of pure $CD4^+$ and the rest were around 1% of $CD8^+$ and around 6% of B cells and macrophages.

2.5. In vitro generation of dendritic cells

Dendritic cells (DC) were obtained from progenitor bone marrow cells of NOD mice. Femur was isolated and flushed aseptically with RPMI1640 + 10% FBS. Cells were then centrifuged, erythrocytes lysed with RBC lysis buffer and cells resuspended in RPMI1640 supplemented with 20% FBS, 2 mM L-glutamine and 1 mM Na-pyruvate. Obtained cells were cultivated with 20 ng/ml GM-CSF (Peprotech, London, UK) for 7 days with medium change every second day. To induce mature DC (mDC), on day 7 cells were treated with maturation stimuli, 100 ng/ml LPS for 24 h. To induce tolerogenic DC (tolDC), treatment with vitamin D3 was performed (2 nM) on days 0, 2, 4 and 6. These cells were also stimulated with LPS on day 7. After maturation, cells were then washed, collected with acutase (ThermoFisher) treatment and seeded at 50,000 cells/well in 96-well U plate (Sardstedt). DCs were treated with $InsB_{9:23}$ peptide (10 μg/ml) (GenScript, Piscataway, NJ, USA) for 4 h before adding $CD4^+$ cell.

2.6. Co-culture of $CD4^+$ and DC

Purified $CD4^+$ cells (500,000) were cultured in 96-well U plate with mature DC (50,000) pre-loaded with $InsB_{9:23}$ peptide either in T lymphocyte medium (previously described X-VIVO™15) or DC medium (previously described RPMI1640). The cells were incubated up to 6 days at 37 °C in the atmosphere with 5% CO_2.

2.7. Insulin-specific cell sorting

After 48 h co-culture with DC, $CD4^+$ cells were stained with PE-conjugated MHC II tetramer of I-A(g7) bound to $InsB_{9–23}$ (HLVERLYL-VAGEEG) or with PE-conjugated human CLIP peptide-containing negative control (PVSKMRMATPLLMQA) (obtained from the National Institutes of Health Tetramer Core Facility at Emory University, New York, USA). Cells were incubated in tetramer solution in pure RPMI1640 with the addition of Fc Block (antiCD16/32 antibody - eBioscience) for 30 min at 37 °C. Subsequently, cells were stained in PBS + 1% BSA containing anti-CD4 PE-Cy7, anti-CD8 APC-Cy7, anti-B220 FITC, anti-F4/80 FITC (eBioscience) for exclusion or potential contaminating cells. Following staining procedure cells were resuspended in culture medium up to 10^7/ml, and separated according to the surface marker expression on FACS Aria III flow cytometer (BD Biosciences, San Jose, CA), using FACSDiva software. The following gating strategy was employed: FSC/SSC gate was used to exclude debris, doublets were eliminated by FSC-A/FSC-W gate, and the insulin-specific $CD4^+$ cells were identified as $B220^-CD8^-CD4^+$ Tet^+.

2.8. Incubation of sorted insulin-specific $CD4^+$ cells

Sorted insulin-specific $CD4^+$ cells were cultured for further 48 h in the presence of TCR stimulators (plate-bound anti-CD3 and soluble anti-CD28 antibody), TGF-β and IL-2. After 48 h cells were stained with anti-CD4 PE-Cy7and anti-CD25 PE, and then sorted as $CD4^+CD25^{high}$ (Treg) or $CD4^+CD25^-$ (Teff) for functional analysis. Polyclonal Treg were also sorted from the *ex vivo* purified $CD4^+$ cells as $CD4^+CD25^{high}$.

Pure insulin-specific $CD4^+$ cells were incubated in the presence of TCR stimulators and IL-2 in combination with rapamycine (100 nM), 5-aza 3'deoxycytidine (1 μM) or STAT-3 inhibitor (10 μg/ml). The proportion of Treg was examined after different time points by flow cytometry.

Pure insulin-specific Treg (obtained after 48 h incubation with TCR stimulators TGF-β and IL-2) were cultured with mature DC (50,000/well) and their number was monitored after 48 h of incubation.

2.9. In vitro suppression assay

For the suppression assay, $CD4^+CD25^-$ cells (effector cells) were

sorted and incubated with 2 μM carboxyfluorescein succinimidyl ester (CFSE) (Invitrogen) for 20 min at RT and 5 min at 37 °C, washed with PBS and resuspended in the T lymphocyte medium. mDC were seeded at 5000 cells/well in U-bottom 96-well plate (Sardstedt, Numbrecht, Germany) in X-VIVO™ 15 in the presence of soluble anti-mouse CD3 (1 μg/ml, eBioscience), and an equal number of purified $CD4^+CD25^-$ cells (25×10^3) was placed in each well. Insulin-specific Treg or polyclonal Treg ($CD4 + CD25^{high}$) were then added in a series of dilutions, starting from 25×10^3 cells per well, and continuing to a 2×, 4×, 8× and 16× lesser number of cells. Certain wells contained only $CD4^+CD25^-$ cells, as control. After 3 days of cultivation, the cells were washed, resuspended in PBS and their division was analyzed by CFSE dilution by flow cytometry.

2.10. Detection of extracellular and intracellular markers by flow cytometry

Surface molecules were detected on viable cells dispersed in PBS + 1% BSA. The following antibodies were used: anti-mouse CD4 PerCP-Cyanine5.5 (rat IgG2a,κ), anti-mouse CD4-FITC (rat IgG2b,κ), CD4-APC (rat IgG2b,κ), anti-mouse CD8-PE (rat IgG2a,κ), anti-mouse B220-FITC (rat IgG2a,κ), CD11c-PE-Cy5 (Armenian hamster IgG), F4/80-FITC (rat IgG2a,κ), CD25-Alexa Fluor® 488 (rat IgG1,λ), CD25-PE (rat IgG1,λ), CD127 APC-eFluor 780 (rat IgG2a,κ), CD357 (GITR)-FITC (rat IgG2b,κ), PD-1-FITC (rat IgG2a,κ), CXCR3-PE (Armenian hamster IgG), CD39-PE (rat IgG2b, κ), CTLA-4-PE (Armenian hamster IgG) (eBioscience). The staining was performed for 30 min at 4 °C. Intracellular staining of IL-10 (FITC-conjugated rat IgG2b, κ - eBioscience) and TGF-β (rabbit anti-mouse + ZyMAX goat anti-rabbit FITC – Thermo Fisher Scientific, Waltham, MA, USA) was performed after 4 h long incubation with Cell Stimulation cocktail that includes phorbol 12-myristate 13-acetate (PMA), ionomycin and brefeldin (eBioscience) in the incubator at 37 °C with 5% CO_2. Cells were first stained with insulin-specific tetramers and then subjected to fixation with 2% paraformaldehyde on room temperature (20 min). Fixed cells were washed in the Permeabilization buffer (eBioscience) and stained with the appropriate antibodies. Regulatory T cells (Treg) were detected by Mouse Regulatory T cell Staining Kit (FoxP3) according to the manufacturer's instructions (eBioscience). Isotype-matched controls were included in all experiments (eBioscience). For Ki67-FITC (goat polyclonal antibody) (SantaCruz Biotechnology, San Diego, USA), cells were permeabilized using the same protocol as for FoxP3 (Treg) detection. Cells were acquired on Partec CyFlow Space by FlowMax software (Partec, Görlitz, Germany) or by BD FACSAria III (BD Biosciences) and analyzed by FlowMax (Partec) or FlowJo software (Treestar, Ashland, OR, USA). Cells were first gated on live cells (empirically determined) and then further gated appropriately to the required analysis.

2.11. ELISA

Supernatants were collected from the culture after *in vitro* suppression assay and used for the determination of cytokines by sandwich ELISA using MaxiSorp plates (Nunck, Rochild, Denmark) and anti-mouse paired antibodies raised against IL-17 or IL-10 (eBioscience) according to the manufacturer's instructions. The final absorbance was measured by LKB microplate reader (LKB Instruments, Vienna, Austria) at 450 and 570 nm. A standard curve created from the known concentrations of appropriate recombinant cytokines was used to calculate concentration values of measured cytokines.

2.12. Statistical analysis

Data are presented as mean ± SD. The presented results are representative of four repeated experiments with comparable results. The significance of differences between groups was determined by two-tailed Student's *t*-test. Differences are regarded as statistically significant if $p < 0.05$. Statistical analyses were performed using GraphPad Prism 5 software (GraphPad Software, Inc., La Jolla, CA, USA).

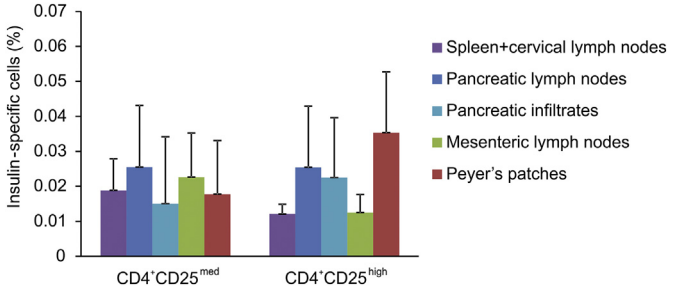

Fig. 1. Insulin-specific $CD4^+$ cells distribution in lymphoid tissues in NOD mice. Insulin-specific conventional $CD4^+CD25^{med}$ and Treg ($CD4^+CD25^{high}$) cells were detected in spleen, cervical, pancreatic and mesenteric lymph nodes, pancreatic infiltrates and Peyer's patches of 2-months old prediabetic NOD mice.

3. Results

3.1. Insulin-specific $CD4^+$ T cell distribution

Insulin-specific $CD4^+$ T lymphocytes are uniformly distributed in the lymphoid tissue of 2 months old prediabetic NOD mice. In addition to the pancreatic lymph nodes and pancreatic infiltrates, these cells were easily detectable in the spleen and cervical lymph nodes as well as within the gut-associated lymphoid tissue (mesenteric lymph nodes and Peyer's patches). The proportion of conventional insulin-specific T cells ($CD4^+CD25^{med}$) compared to insulin-specific Treg ($CD4^+CD25^{high}$) is slightly higher in spleen and mesenteric lymph nodes, the proportions of these two populations were more or less equal in the pancreatic lymph nodes and pancreatic infiltrates while in Peyer's patches insulin-specific Treg predominate (Fig. 1).

3.2. Ex vivo insulin-specific $CD4^+$ cells enrichment

Since autoantigen-specific Treg cells are extremely difficult to isolate from the whole blood (in the case of human source) (Pihl et al., 2017) or from the rodent lymphoid tissues (spleen, cervical, mesenteric or pancreatic lymph nodes, or Peyer's patches) due to the very low numbers (Fig. 1), we have set out to explore different modes for insulin-specific Treg expansion *in vitro*. In order to get higher numbers of insulin-specific T cells, purified $CD4^+$ cells were incubated in the presence of mDC previously loaded with insulin B chain peptide ($InsB_{9:38}$). The initial experiments proved low presence of other cell contaminants in the purified population of $CD4^+$ (purity was around 95%). After 48–72 h of incubation, the proportion (Fig. 2A) and the number (Fig. 2B) of insulin-specific $CD4^+$ cells was the highest. The proportion of insulin-specific $CD4^+$ cells varied from 1.9% up to 8.1% depending upon the experiment (Fig. 2C). The best viability of $CD4^+$ cells in co-culture with mDC was obtained when cells were incubated in X-VIVO™15 supplemented with 10% FBS and in the absence of additional IL-2 (Fig. 2D).

Phenotypic determination of insulin-specific cells revealed that Treg ($CD4^+CD25^{high}$) population increased over time while the proportion of insulin-specific T effector cells ($CD4^+CD25^{med}$) stagnated (Fig. 2E). Moreover, this trend of insulin-specific Treg increase was similar when tolDC were used (Fig. 2F).

3.3. The function of insulin-specific Treg

The *in vitro* gained insulin-specific $CD4^+$ cells were sorted and cultured in the presence of Treg cocktail (plate-bound anti-CD3

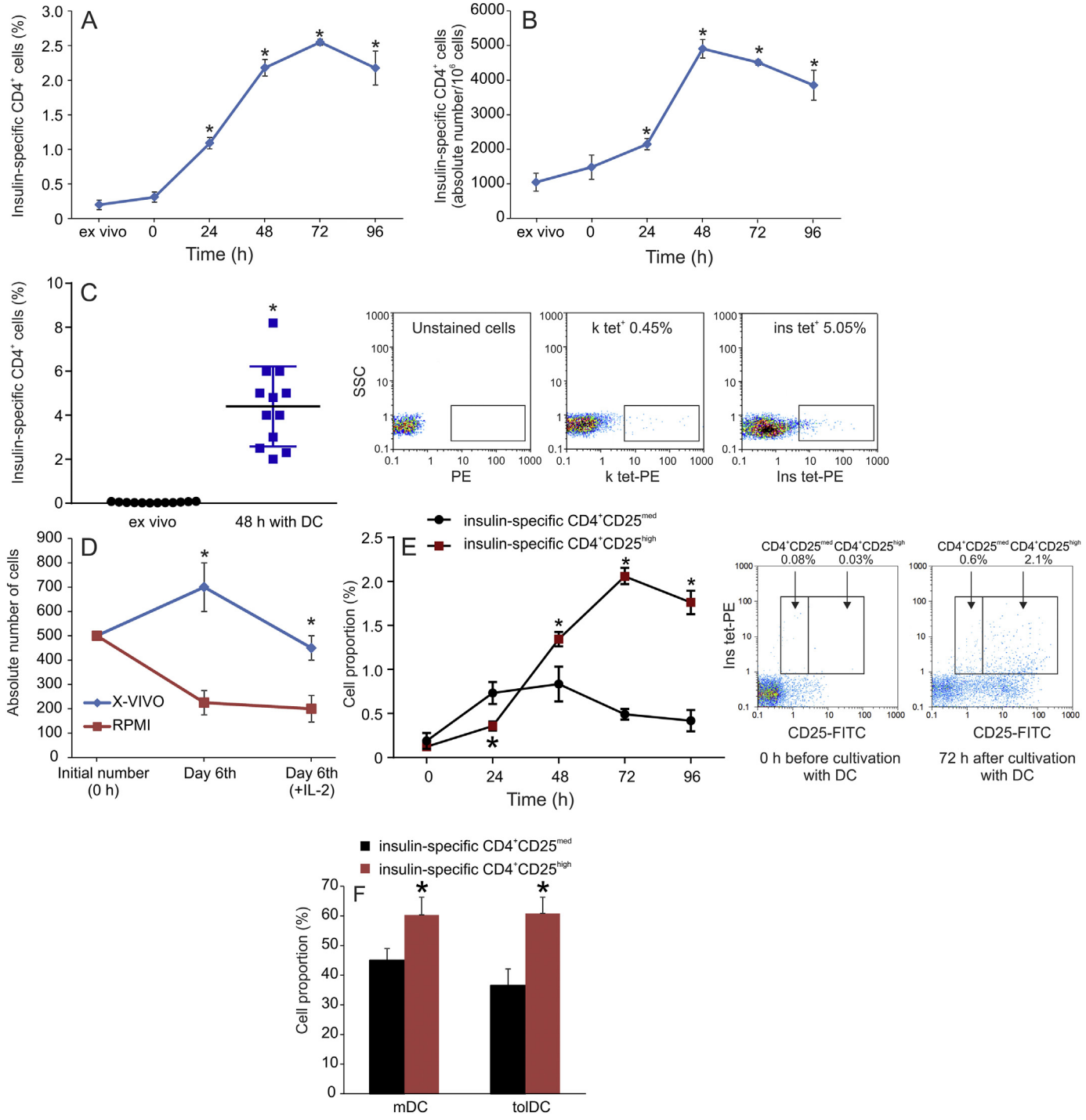

Fig. 2. Enrichment of insulin-specific T cells. The proportion (A) and absolute number (B) of insulin-specific $CD4^+$ cells after co-culture of pure $CD4^+$ and mature $InsB_{9:23}$-loaded DC. The proportion of insulin-specific $CD4^+$ cells after 48 h of co-culture (C). The representative dot plots are presented on the right-hand side. Cells were first gated on live cells and then the proportion of control tetrames-stained and insulin-tetramer-stained cells was determined. The absolute number of $CD4^+$ cells in co-culture with mature $InsB_{9:23}$-loaded DC in X-VIVO™ 15 or RPMI1640 medium (the composition of medium is described in Material and Methods) in the presence or absence of additional IL-2 (10 ng/ml) after 6 days of incubation (D). The proportion of effector $CD4^+CD25^{med}$ and Treg ($CD4^+CD25^{high}$) within insulin-specific T cells during co-culture with mature $InsB_{9:23}$-loaded DC (E). The representative dot plots of cells after 48 h of incubation are presented on the right-hand side. The proportion of effector $CD4^+CD25^{med}$ and Treg ($CD4^+CD25^{high}$) within insulin-specific T cells during co-culture with mature (m) or tolerogenic (tol) $InsB_{9:23}$-loaded DC after 48 h of incubation (F). $*p < 0.05$ represents a statistically significant difference between different time points and the beginning of culture (A, B, C), or between samples in X-VIVO™ 15 and RPMI1640 medium (D), or between the proportion of $CD4^+CD25^{high}$ and $CD4^+CD25^{med}$ cells (E, F).

antibody, soluble anti-CD28 antibody, recombinant IL-2 and TGF-β). After 48 h, the outcome was almost 100% pure $CD4^+CD25^{high}FoxP3^+$ (Fig. 3A). These cells were subjected to different assays to test their suppressive properties. First of all, they exhibited full Treg phenotype through expression of glucocorticoid-induced TNFR family related (GITR) and lack of CD127 surface molecule (Fig. 3B).

Further, they produced IL-10 and TGF-β in culture and the production of these cytokines increased over time (Fig. 4A and B). The proportion of insulin-specific IL-10^+ cells was 10.5 ± 1.2%, while TGF-β^+ was 27.3 ± 2.6%. Insulin-specific Treg successfully blocked T

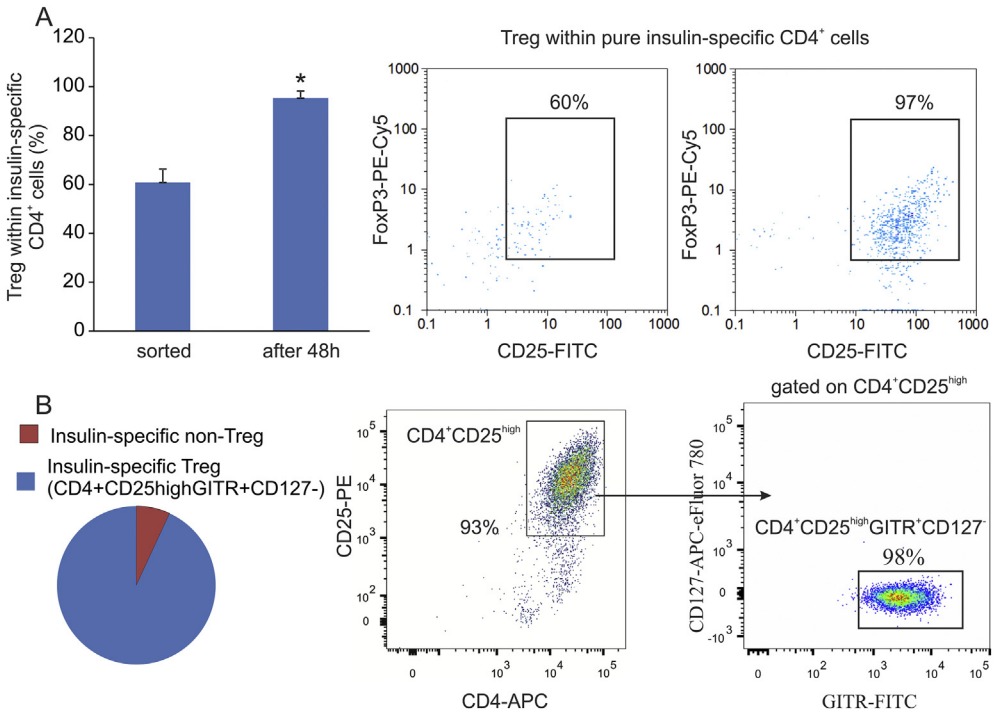

Fig. 3. Purification of insulin-specific Treg in culture. The proportion of insulin-specific Treg within insulin-specific T cells sorted after 48 h co-culture with mature DC (sorted) or after culture of sorted cells with TCR stimulators in the presence of IL-2 (10 ng/ml) and TGF-β (2 ng/ml). (A). Representative dot plots of $CD25^{high}FoxP3^{+}$ insulin-specific cells are shown at the right-hand side. The presence of CD127 and GITR on $CD4^{+}CD25^{high}$ insulin-specific T cells after 48 h with TCR stimulators in the presence of IL-2 (10 ng/ml) and TGF-β (2 ng/ml) (B).

effector cell proliferation in the suppression assay and were more potent than polyclonal Treg (Fig. 4C). Along with the inhibition of IL-17 production (Fig. 4D), the amount of TGF-β was significantly up-regulated (Fig. 4E). The inhibitory molecule CD39 was present on > 60% of Treg population, PD-1 was found on the half of Treg, while CTLA-4 was expressed in around 8% of Treg. The expression of CXCR3 was found on almost all insulin-specific Treg (Fig. 4F).

3.4. Expansion of sorted insulin-specific Treg

The further expansion of insulin-specific Treg was tested in the cell-free system or in the presence of mDC. Cell-free system implies the stimulation of cells with plate-bound anti-CD3 antibody and soluble anti-CD28 antibody in the presence of IL-2. In this setting, insulin-specific Treg did not engage in further proliferation and after 72 h, they started to lose Treg phenotype. The simultaneous application of rapamycine (mTOR inhibitor and stimulator of Treg proliferation) or 5-aza 3′deoxycitidine (demethylating agent that promotes FoxP3 expression) were not able to stabilize the Treg phenotype (Fig. 5A). In addition, STAT3 inhibitor (inhibitor of Th17 cell differentiation) partly maintained Treg phenotype of insulin-specific cells after 5 days of incubation (Fig. 5A). The best results were obtained when mDC were used, *i.e.* the presence of mDC (along with soluble anti-CD3 antibody and IL-2) had stimulating influence on Treg proliferation (Fig. 5B).

4. Discussion

This study provides new experimental design for the enrichment and expansion of insulin-specific Treg that can be used for the cell-based therapy of autoimmunity. This protocol implies the usage of mature dendritic cells both in the phase of Treg enrichment and in the phase of Treg expansion.

Autoantigen-specific Treg are extremely rarely found in the blood and lymphoid tissues, but have been shown to possess significant potential for inhibition of autoantigen-specific T effector cells. For example, as low as 5000 BDC 2.5-specific Treg were enough to delay the T1D transfer in BDC 2.5 transgenic NOD mice. All autoantigen-specific Treg that have been investigated for T1D treatment were transgenic, either they come from the animal that expresses the specific TCR for autoantigen, or T cells were engineered *via* transfection of viral vectors encoding specific T cell receptors (TCRs) or chimeric antigen receptors (CARs) (Zhang et al., 2018). We have chosen to try to expand insulin-specific Treg because insulin is the key autoantigen for driving the initiation and progression of autoimmune beta cell destruction (Nakayama et al., 2005; Nakayama et al., 2007; Jaeckel et al., 2004). The potency of innate insulin-specific Treg in the combat against T1D is represented by the fact that high frequency of these cells were found in the blood of prediabetic subjects that have long history of anti-islet autoimmunity compared to healthy subjects and those with diabetes onset at a young age (Serr et al., 2016). Our results suggest that insulin-specific Treg can be found in all lymphoid tissues in NOD mice. Also, the observations made by Spence et al. about the higher frequency insulin-specific Treg compared to the conventional T cells within the pancreatic infiltrates was confirmed in this study (Spence et al., 2018).

The kinetics of insulin-specific Treg proliferation during encounter with the $InsB_{9:23}$-loaded DC showed that these cells were significantly more expanding compared to the conventional insulin-specific T lymphocytes. This preference for Treg expansion was not surprising, as previously published observations suggest that mature DCs were able to stimulate Treg differentiation from naïve $CD4^{+}CD25^{-}$ cells (Banerjee et al., 2006). Surprisingly, tolDCs were equally efficient in promoting insulin-specific Treg as were mature DCs. Hypothetically, this can be due to the fact that in the “normal” system, the proliferation of effector T cells to the self- antigen is limited, and even mature DC have the capacity to promote autoantigen-specific Treg.

Treg obtained by *in vitro* enrichment were fully functional since they exhibited suppressive effect on T efector cells. Most importantly, these Treg had higher inhibitory influence compared to polyclonal, freshly isolated $CD4^{+}CD25^{high}$ Treg cells suggesting that their action is specific and more focused. Also, the fact that smaller number of insulin-specific Treg was effective suggests their higher potency. This was also documented in the literature when as little as 5000 BDC2.5-specific Treg were used to halt T1D in the transfer model of the disease, compared to 10^{5} polyclonal Treg (Tarbell et al., 2004). Treg exhibit their inhibitory effect on T cell proliferation either through cell contact (by expression of various surface molecules including GITR and CTLA-4) (Kumar et al.,

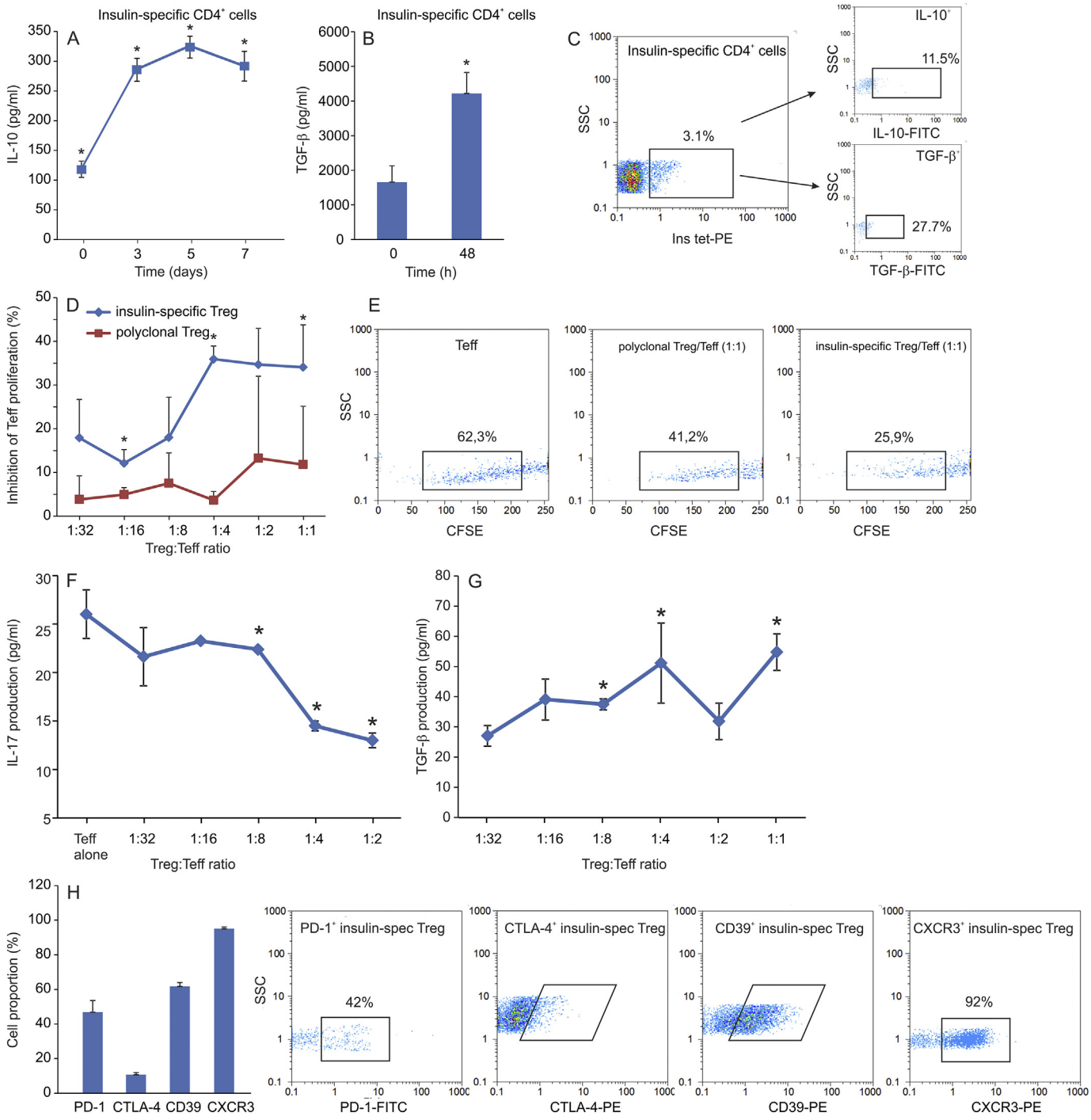

Fig. 4. The function of insulin-specific Treg expanded in culture. Production of IL-10 (A) and TGF-β (B) in the culture of sorted insulin-specific CD4$^+$ cells with TCR stimulators in the presence of IL-2 (10 ng/ml) and TGF-β (2 ng/ml). IL-10$^+$ and TGF-β$^+$ population within insulin-specific cells (C). Polyclonal Treg and insulin-specific cells capacity of inhibition of T effector cell (Teff) proliferation measured by CFSE dilution in *in vitro* suppression assay (D). (E) Representative dot plots of CFSE dilution that represents the proliferation of Teff are shown (Teff/Treg ratio was 1:1). IL-17 (F) and TGF-β (G) secretion during *in vitro* suppression assay. (H) CD39$^+$, PD-1$^+$, CTLA-4$^+$ and CXCR3$^+$ proportion within insulin-specific Treg cells after 48 of culture with TCR stimulators in the presence of IL-2 (10 ng/ml) and TGF-β (2 ng/ml). *$p < 0.05$ represents a statistically significant difference between secretion of IL-10 and TGF-β over time compared to the starting point of culture (0) (A, B), or the difference between the effects of polyclonal *vs* insulin-specific Treg (D, E), or IL-17 and TGF-β production between Teff + Treg cultures and those with Teff alone (F, G).

2018) or by secretion of immunosuppressive cytokines (Yu et al., 2018). Also, Treg express on their surface ecto-nucleotidase CD39 that converts ATP to adenosine, an immunosuppressive molecule (Dwyer et al., 2007). The expanded insulin-specific Treg probably used versatile ways for suppression: inhibition by cell-to-cell contact through GITR (and to smaller extent through CTLA-4), soluble factors (IL-10 and TGF-β) and through generation of adenosine in the extracellular milieu.

Migratory properties of Treg are extremely important for the potential *in vivo* application. Therefore, the observed expression of CXCR3 on almost all obtained insulin-specific Treg is crucial for directing cells into the inflamed tissue (in this case pancreatic islets). CXCR3 responds to CXCL9, CXCL10 and CXCL11 that are highly expressed during

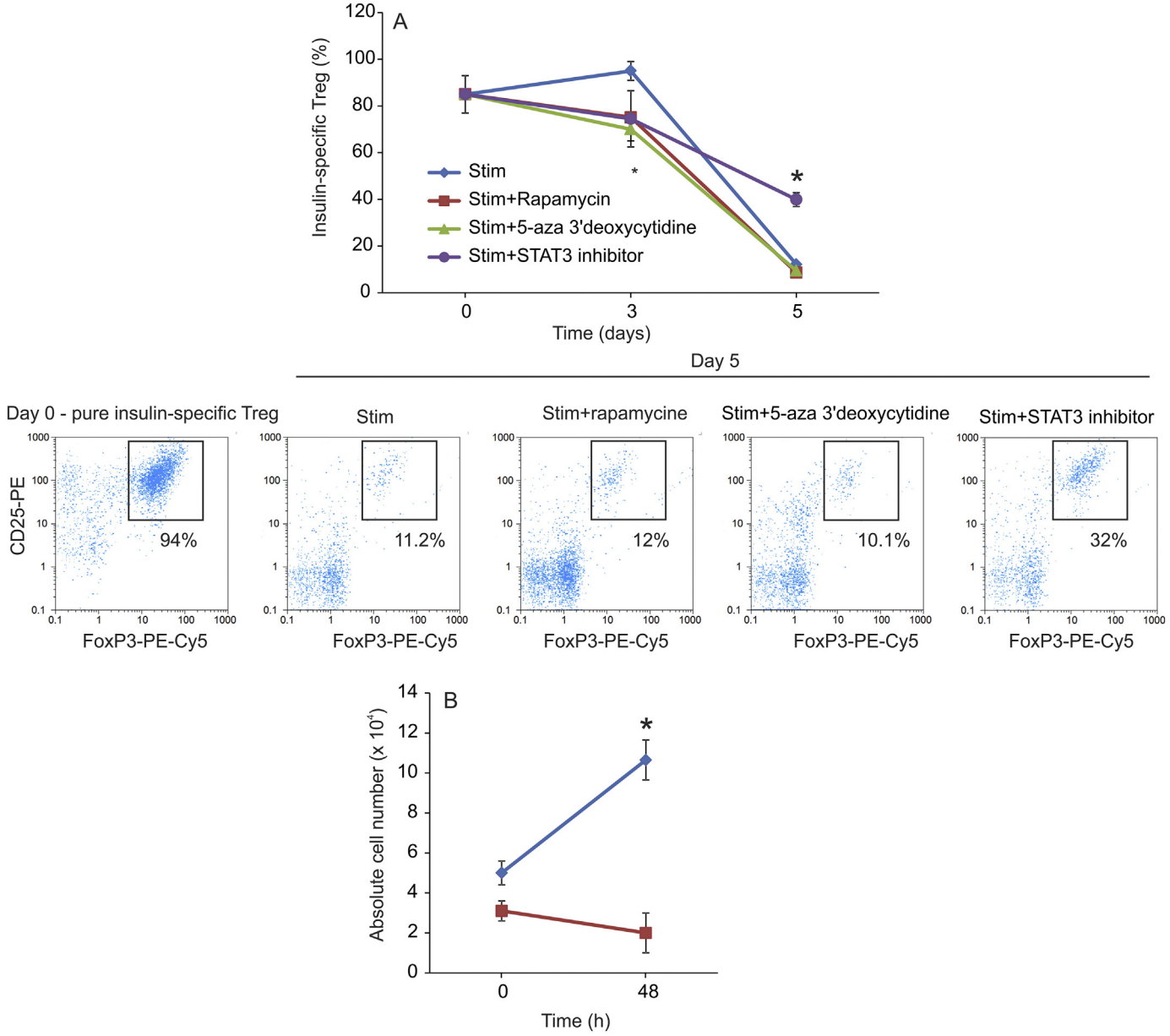

Fig. 5. Expansion of insulin-specific Treg. The proportion of insulin-specific Treg after incubation with TCR stimulators and IL-2 (Stim) and in the combination with rapamycine (100 nM), 5-aza3'deoxycytidine (1 μM), or STAT3 inhibitor (10 μg/ml) (A). The representative dot plots are shown below and present the proportion of FoxP3^{+}CD25^{high} cells. The absolute number of pure insulin-specific Treg cultured in the cell-free system with TCR stimulation and IL-2, or in the presence of mature DC (mDC) and anti-CD3 antibody (1 μg/ml) and IL-2 (10 ng/ml) (B). *$p < 0.05$ represents a statistically significant difference between stimulated culture and those treated with various modulators (A) or difference between absolute cell number after 48 h of incubation compared to point 0 (B).

inflammation (Groom and Luster, 2011).

Further expansion of pure insulin-specific Treg was dependent upon the presence of direct cell contact with DC. The ever-present problem for *in vitro* expanded or generated Treg is their potential reversion to the inflammatory phenotype (Ren and Li, 2017). The observed destabilization of insulin-specific Treg phenotype in the absence of supporting cells was partly ameliorated by the addition of STAT3 inhibitor that blocks Th17 differentiation (Chen and Laurence, 2007). Treg conversion into Th17 is well-documented and it happens because these cells share the same progenitor and the cytokine requirements for their differentiation are very similar (Ren and Li, 2017). The absence of the supporting effect for rapamycine and 5-aza 3'deoxycytdine was in contrast to the previously published studies. Specifically, rapamycine is known to stimulate Treg proliferation by blocking mTOR pathway (Battaglia et al., 2005; Hou et al., 2018), while 5-aza 3′deoxycytdine through demethylation of FoxP3 promotor stabilizes long-term FoxP3 expression (Freudenberg et al., 2018). This discrepancy may be a result of already optimal engaged signalling pathways (through TCR and IL-2) that lead to FoxP3 expression, and therefore the addition of stimulators has no further impact on proliferation or gene expression.

In conclusion, *in vitro* generation of insulin-specific Treg is a three-stage protocol and it consists of: enrichment stage where insulin-specific CD4^{+} cells are expanded in the presence of cellular signal from mDC, purification stage where sorted insulin-specific CD4^{+} are subjected to TCR signal, IL-2 and TGF-β and the only population that survives is insulin-specific Treg population, and finally expansion stage where again in the presence of mDC, insulin-specific Treg proliferate (Fig. 6). The obtained insulin-specific Treg are fully functional and this protocol repeatedly provided sufficient numbers of Treg needed for the future *in vivo* application in the mouse model of T1D.

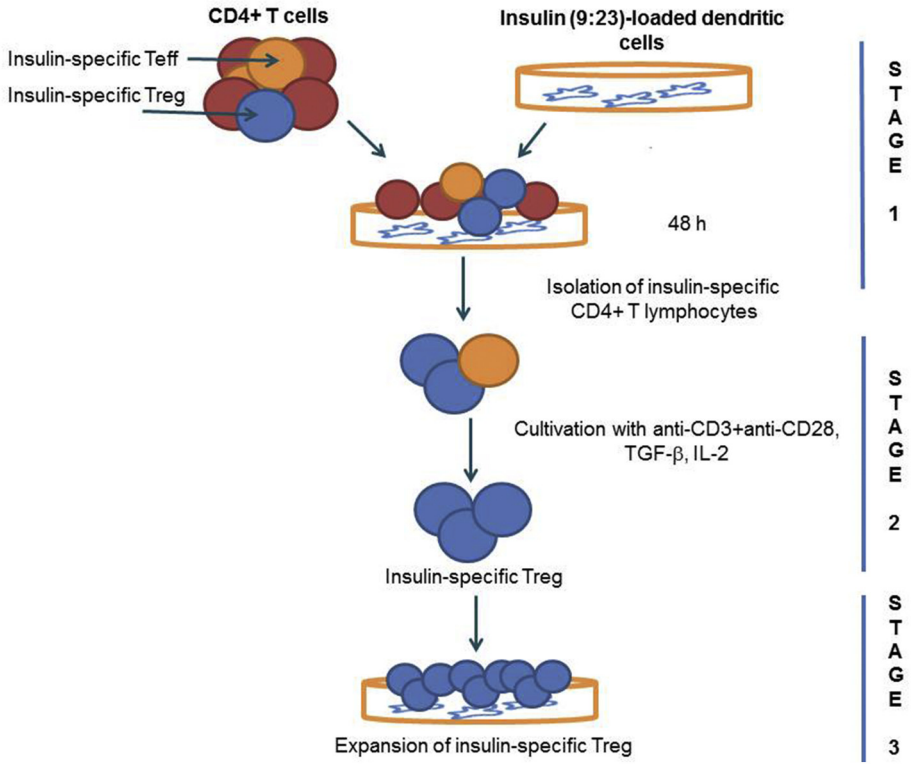

Fig. 6. Schematic work-flow of the protocol for the enrichment (stage 1), purification (stage 2) and expansion (stage 3) of insulin-specific Treg.

Acknowledgment

We would like to thank Dr. Milica Vujičić, Dr. Tamara Saksida and Ivan Koprivica (Institute for Biological Research "Siniša Stanković", University of Belgrade) for useful comments and discussions.

Funding

This work was supported by The Iacocca Family Foundation, Boston, MA, USA and partly by the Ministry of Education, Science and Technological Development, Republic of Serbia (grant No: 173013).

References

Banerjee, D.K., Dhodapkar, M.V., Matayev,a, E., Steinman, R.M., Dhodapkar, K.M., 2006. Expansion of FOXP3high regulatory T cells by human dendritic cells (DCs) in vitro and after injection of cytokine-matured DCs in myeloma patients. Blood 108, 2655–2661.

Battaglia, M.A., Stabilini, M., Roncarolo, G., 2005. Rapamycin selectively expands $CD4^+CD25^+FoxP3^+$ regulatory T cells. Blood 105, 4743–4748.

Bluestone, J.A., Buckner, J.H., Fitch, M., Gitelman, S.E., Gupta, S., Hellerstein, M.K., Herold, K.C., Lares, A., Lee, M.R., Li, K., Liu, W., Long, S.A., Masiello, L.M., Nguyen, V., Putnam, A.L., Rieck, M., Sayre, P.H., Tang, Q., 2015. Type 1 diabetes immunotherapy using polyclonal regulatory T cells. Sci. Transl. Med. 7, 315ra189.

Chen, Z., Laurence, A., O'Shea, J.J., 2007. Signal transduction pathways and transcriptional regulation in the control of Th17 differentiation. Semin. Immunol. 19, 400–408. https://doi.org/10.1016/j.smim.2007.10.015.

Dwyer, K.M., Deaglio, S., Gao, W., Friedman, D., Strom, T.B., Robson, S.C., 2007. CD39 and control of cellular immune responses. Purinergic Signal 3, 171–180. https://doi.org/10.1007/s11302-006-9050-y.

Freudenberg, K., Lindner, N., Dohnke, S., Garbe, A.I., Schallenberg, S., Kretschmer, K., 2018. Critical role of TGF-β and IL-2 receptor signaling in Foxp3 induction by an inhibitor of DNA methylation. Front. Immunol. 9, 125. https://doi.org/10.3389/fimmu.2018.00125.

Groom, J.R., Luster, A.D., 2011. CXCR3 in T cell function. Exp. Cell Res. 317, 620–631. https://doi.org/10.1016/j.yexcr.2010.12.017.

Hou, H., Cao, R., Quan, M., Sun, Y., Sun, H., Zhang, J., Li, B., Guo, L., Song, X., 2018. Rapamycin and fingolimod modulate Treg/Th17 cells in experimental autoimmune encephalomyelitis by regulating the Akt-mTOR and MAPK/ERK pathways. J. Neuroimmunol. 324, 26–34. https://doi.org/10.1016/j.jneuroim.2018.08.012.

Jaeckel, E., Lipes, M.A., von Boehmer, H., 2004. Recessive tolerance to preproinsulin 2 reduces but does not abolish type 1 diabetes. Nat. Immunol. 5, 1028–1035.

Kumar, P., Bhattacharya, P., Prabhakar, B.S., 2018. A comprehensive review on the role of co-signaling receptors and Treg homeostasis in autoimmunity and tumor immunity. J. Autoimmun. 95, 77–99. https://doi.org/10.1016/j.jaut.2018.08.007.

Liu, W., Putnam, A.L., Xu-Yu, Z., Szot, G.L., Lee, M.R., Zhu, S., Gottlieb, P., Kapranov, P., Gingeras, T.R., Fazekas de St Groth, B., Clayberger, C., Soper, D.M., Ziegler, S.F., Bluestone, J.A., 2006. CD127 expression inversely correlates with FoxP3 and suppressive function of human $CD4^+$ T reg cells. J. Exp. Med. 203, 701–711.

Marek-Trzonkowska, N., Mysliwiec, M., Dobyszuk, A., Grabowska, M., Techmanska, I., Juscinska, J., Wujtewicz, M.A., Witkowski, P., Mlynarski, W., Balcerska, A., Mysliwska, J., Trzonkowski, P., 2012. Administration of $CD4^+CD25^{high}CD127^-$ regulatory T cells preserves b-cell function in type 1 diabetes in children. Diabetes Care 35, 1817–1820.

Marek-Trzonkowska, N., Myśliwiec, M., Dobyszuk, A., Grabowska, M., Derkowska, I., Juścińska, J., Owczuk, R., Szadkowska, A., Witkowski, P., Młynarski, W., Jarosz-Chobot, P., Bossowski, A., Siebert, J., Trzonkowski, P., 2014. Therapy of type 1 diabetes with $CD4^+CD25^{high}CD127^-$ regulatory T cells prolongs survival of pancreatic islets - results of 1 year follow-up. Clin. Immunol. 153, 23–30.

Masteller, E.L., Warner, M.R., Tang, Q., Tarbell, K.V., McDevitt, H., Bluestone, J.A., 2005. Expansion of functional endogenous antigen-specific $CD4^+CD25^+$ regulatory T cells from nonobese diabetic mice. J. Immunol. 175, 3053–3059.

Milward, K.F., Wood, K.J., Hester, J., 2017. Enhancing human regulatory T cells in vitro for cell therapy applications. Immunol. Lett. 190, 139–147.

Nakayama, M., Abiru, N., Moriyama, H., Babaya, N., Liu, E., Miao, D., Yu, L., Wegmann, D.R., Hutton, J.C., Elliott, J.F., Eisenbarth, G.S., 2005. Prime role for an insulin epitope in the development of type 1 diabetes in NOD mice. Nature 435, 220–223.

Nakayama, M., Beilke, J.N., Jasinski, J.M., Kobayashi, M., Miao, D., Li, M., Coulombe, M.G., Liu, E., Elliott, J.F., Gill, R.G., Eisenbarth, G.S., 2007. Priming and effector dependence on insulin B:9-23 peptide in NOD islet autoimmunity. J. Clin. Invest. 117, 1835–1843.

Pihl, M., Barcenilla, H., Axelsson, S., Chéramy, M., Åkerman, L., Johansson, I., Ludvigsson, J., Casas, R., 2017. GAD-specific T cells are induced by GAD-alum treatment in Type-1 diabetes patients. Clin. Immunol. 176, 114–121. https://doi.org/10.1016/j.clim.2017.01.010. (Mar).

Ren, J., Li, B., 2017. The functional stability of FOXP3 and RORγt in Treg and Th17 and their therapeutic applications. Adv. Protein Chem. Struct. Biol. 107, 155–189. https://doi.org/10.1016/bs.apcsb.2016.10.002.

Serr, I., Fürst, R.W., Achenbach, P., Scherm, M.G., Gökmen, F., Haupt, F., Sedlmeier, E.M., Knopff, A., Shultz, L., Willis, R.A., Ziegler, A.G., Daniel, C., 2016. Type 1 diabetes vaccine candidates promote human Foxp3(+)Treg induction in humanized mice. Nat. Commun. 7, 10991.

Spence, A., Purtha, W., Tam, J., Dong, S., Kim, Y., Ju, C.H., Sterling, T., Nakayama, M., Robinson, W.H., Bluestone, J.A., Anderson, M.S., Tang, Q., 2018. Revealing the specificity of regulatory T cells in murine autoimmune diabetes. Proc. Natl. Acad. Sci. U. S. A. 115, 5265–5270. https://doi.org/10.1073/pnas.1715590115.

Stojanovic, I., Dimitrijevic, M., Vives-Pi, M., Mansilla, M.J., Pujol-Autonell, I., Rodríguez-Fernandez, S., Palova-Jelínkova, L., Funda, D.P., Gruden-Movsesijan, A., Sofronic-

Milosavljevic, L., Hilkens, C.M.U., Martinez-Caceres, E., Miljkovic, D., 2017. Cell-based Tolerogenic therapy, experience from animal models of multiple sclerosis, Type 1 diabetes and rheumatoid arthritis. Curr. Pharm. Des. 23, 2623–2643. https://doi.org/10.2174/1381612823666170214120708.

Tang, Q., Lee, K., 2012. Regulatory T-cell therapy for transplantation: how many cells do we need? Curr. Opin. Organ Transplant. 17, 349–354.

Tang, Q., Henriksen, K.J., Bi, M., Finger, E.B., Szot, G., Ye, J., Masteller, E.L., McDevitt, H., Bonyhadi, M., Bluestone, J.A., 2004. *In vitro*-expanded antigen-specific regulatory T cells suppress autoimmune diabetes. J. Exp. Med. 199, 1455–1465.

Tarbell, K.V., Yamazaki, S., Olson, K., Toy, P., Steinman, R.M., 2004. $CD25^+CD4^+$ T cells, expanded with dendritic cells presenting a single autoantigenic peptide, suppress autoimmune diabetes. J. Exp. Med. 199, 1467–1477.

Tonkin, D.R., He, J., Barbour, G., Haskins, K., 2008. Regulatory T cells prevent transfer of type 1 diabetes in NOD mice only when their antigen is present *in vivo*. J. Immunol. 181, 4516–4522.

Yu, H., Paiva, R., Flavell, R.A., 2018. Harnessing the power of regulatory T-cells to control autoimmune diabetes: overview and perspective. Immunology 153, 161–170. https://doi.org/10.1111/imm.12867.

Zhang, Q., Lu, W., Liang, C.L., Chen, Y., Liu, H., Qiu, F., Dai, Z., 2018. Chimeric antigen receptor (CAR) Treg: a promising approach to inducing immunological tolerance. Front. Immunol. 9, 2359. https://doi.org/10.3389/fimmu.2018.02359. (eCollection 2018).